# Copolymerization of an Aryl Halide and Elemental Sulfur as a Route to High Sulfur Content Materials

| | |
|---|---|
| Journal: | *Polymer Chemistry* |
| Manuscript ID | PY-ART-11-2019-001706.R1 |
| Article Type: | Paper |
| Date Submitted by the Author: | 03-Jan-2020 |
| Complete List of Authors: | Karunarathna, Menisha; Clemson University, Department of Chemistry<br>Lauer, Moira; Clemson University, Department of Chemistry<br>Tennyson, Andrew; Clemson University, Department of Chemistry<br>Smith, Rhett; Clemson University, Department of Chemistry |
| | |

# Copolymerization of an Aryl Halide and Elemental Sulfur as a Route to High Sulfur Content Materials

*Menisha S. Karunarathna[a], Moira K. Lauer[a], Andrew G. Tennyson,[a,b] and Rhett C. Smith[a]\**

High sulfur-content materials (HSMs) have been investigated for a plethora of applications owing to a combination of desirable properties and the low cost of waste sulfur as a starting monomer. Whereas extended sulfur catenates are unstable with respect to orthorhombic sulfur ($S_8$ rings) at STP, oligomeric / polymeric sulfur chains can be stabilized when they are confined in a supporting matrix. The vast majority of reported HSMs have been made by inverse vulcanization of sulfur and olefins. In the current case, a radical aryl halide-sulfur polymerization (RASP) route was employed to form an HSM (**XS81**) by copolymerizing elemental sulfur with the xylenol derivative 2,4-dimethyl-3,5-dichlorophenol (DDP). **XS81** is a composite of which 81 wt.% is sulfur, wherein the sulfur is distributed between cross-linking chains averaging four sulfur atoms in length and trapped sulfur that is not covalently attached to the network. **XS81** (flexural strength = 2.0 MPa) exhibits mechanical properties on par with other HSMs prepared by inverse vulcanization. Notably, **XS81** retains mechanical integrity over many heat-recast cycles, making it a candidate for facile recyclability. This is the first report of a HSM comprising stabilized polymeric sulfur that has been successfully prepared from a small molecular comonomer by RASP. Preparation of **XS81** thus demonstrates a new route to access HSMs using small molecular aryl halides, a notable expansion beyond the olefins required for the well-studied inverse vulcanization route to HSMs from small molecular comonomers.

## Introduction

Pyun's landmark discovery that high sulfur-content materials (HSMs) can be readily-prepared from olefins by their inverse vulcanization with majority component elemental sulfur (Scheme 1A)[1] has inspired a flurry of research.[2-4] Inverse vulcanization opens new vistas for valorising the >7 million tons of elemental sulfur waste generated annually by the petroleum refining industry. Researchers have leveraged the elegance of the inverse vulcanization procedure to prepare HSMs from a plethora of olefin-bearing comonomers including cyclopentadiene,[5, 6] styrene derivatives,[1, 7-13] vinyl ethers,[14] amino acid derivatives,[15] vegetable oils,[16-20 21, 22] free fatty acids,[23] other plant-derived olefins such as terpenoids,[6, 14, 17, 24-26] lignin,[27] and cellulose.[28] HSMs have demonstrated remarkable application diversity to include infrared imaging camera lenses,[29, 30] lithium-sulfur battery components,[31, 32] absorbents for water purification / oil spill clean-up, [6, 8, 33-35 21] slow-release fertilizers[16, 20] and as cement protectant / replacement materials.[28, 36-41] The thermal reversibility of S–S

bonds further endow HSMs with potential for thermal healing and recyclability by simple melt processing. [13, 23, 42-46]

At STP the eight-membered $S_8$ ring, in the orthorhombic crystal morphology, is the most stable allotrope of elemental sulfur. Above 159 °C, thermally-induced homolytic ring-opening and concomitant homologation occurs to form polymeric sulfur radicals (Scheme 1A). Upon cooling to room temperature, polymeric sulfur catenates are unstable and revert back to orthorhombic sulfur with loss of mechanical integrity. In HSMs produced via inverse vulcanization, however, the polymeric sulfur domains, often characterized by an orange-brown colour (Figure 1A) are confined in a polymeric organosulfur matrix and often do not readily revert back to the orthorhombic state. Because the polymeric sulfur is retained in these HSMs, the mechanical durability characteristic of a polymeric material is retained.

The burgeoning success of HSMs has inspired efforts to develop protocols that would expand the monomer scope beyond the olefins required for inverse vulcanization. The Smith group recently reported radical-induced aryl halide-sulfur polymerization (RASP, Scheme 1B),[47] wherein elemental sulfur reacts with chlorolignin to produce HSMs having polysulfide-bridged aryl rings. In that report, the pre-existing polymer network of lignin facilitates stabilization of polymeric sulfur domains.

[a.] Department of Chemistry and Center for Optical Materials Science and Engineering Technologies, Clemson University, Clemson, South Carolina, United States.
[b.] Department of Materials Science and Engineering, Clemson University, Clemson, South Carolina, United States.

We hypothesized that an appropriately-functionalized small molecular aryl halide could undergo reaction with sulfur to produce a covalently-crosslinked network that could likewise stabilize polymeric sulfur networks to produce HSMs similar to those made by inverse vulcanization.[48-50] Herein, the RASP of 2,4-dichloro-3,5-dimethylphenol (DDP) with elemental sulfur is reported. Durable materials comprising polymeric sulfur trapped within a crosslinked network (**XS81**) were achieved. The composition and thermal / mechanical properties of **XS81** were studied by a combination of elemental analysis, DSC, TGA, and DMA techniques. The formation of direct S–$C_{aryl}$ bonds was confirmed by depolymerizing **XS81** and analysing the depolymerization products using Ellman's reagent. Recyclability of **XS81** (Figure 1B) with complete retention of mechanical strength was confirmed by recursive pulverize-melt-recast cycles followed by dynamic mechanical analysis.
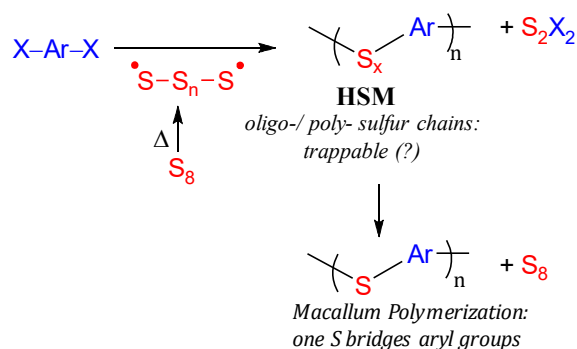
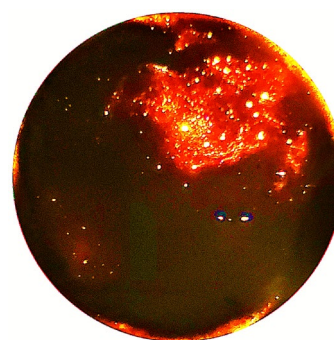A) Inverse Vulcanization (Pyun, 2013): *Requires an Olefin*
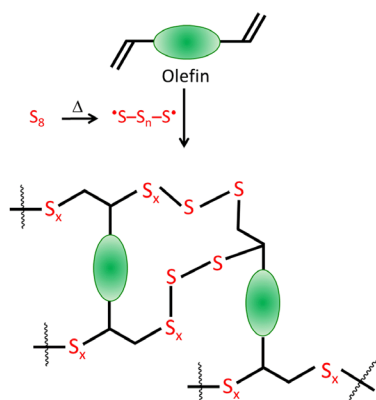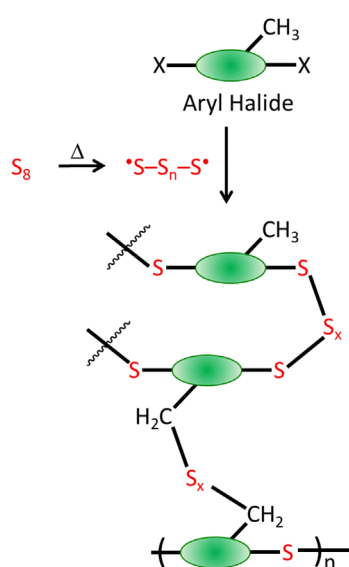
**Scheme 1**. Established inverse vulcanization (A) and new radical-induced aryl halide-sulfur polymerization (RASP) route (B) to (HSMs). Benzylic sites can be crosslinked in either reaction.

**Scheme 2.** Formation of S–$C_{aryl}$ bonds by reaction of sulfur with an aryl halide in Macallum Polymerization or RASP.
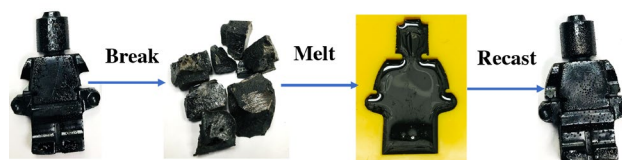
A)

B)

**Figure 1.** A backlit sample of **XS81** illustrates the brown-orange colour characteristic of polymeric sulfur (A). Facile recycling of **XS81** is demonstrated by breaking a sample followed by melt-processing from a silicone mould (B).

## Results and Discussion

### Synthesis and Structure

The inverse vulcanization route to HSMs involves reaction of sulfur with olefins by chemistry similar to Goodyear's classic vulcanization,[51] but in inverse vulcanization sulfur is the majority component rather than the olefin. Likewise, the RASP mechanism (Scheme 2) proceeds via chemistry similar to the classic Macallum route to poly(aryl sulphide) derivatives, but RASP employs an excess of sulfur with respect to the aryl halide. For the current study, 2,4-dichloro-3,5-dimethylphenol (DDP) was selected as the aryl halide. DDP is attractive first because it is readily prepared from an abundant xylyl alcohol, by green reaction with aqueous bleach solution, DDP is currently quite affordable at 1 USD per kilogram (Alibaba pricelist as of this

writing) and because each aryl ring has two chlorides and two benzylic methyl groups that are cross-linkable to afford a network in which polymeric sulfur chains could be stabilized. The presence of the electron-releasing –OH moiety is also advantageous because electron-releasing substituents activate aryl rings for the Macallum reaction.[52]
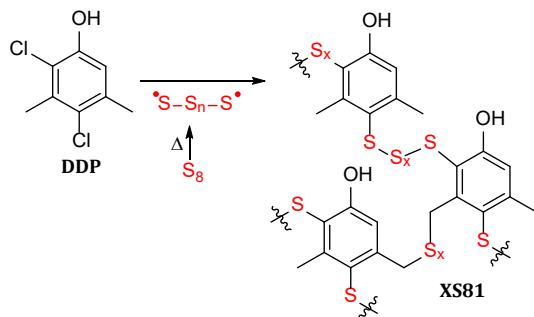


**Scheme 3.** Preparation of **XS81** by RASP. Only the covalently-incorporated sulfur is shown in this structure.

The highest flexural strength for the materials previously prepared by RASP was accomplished in a material having 81 wt% S.[47] For the current study, an initial monomer feed was therefore selected such that the resulting material would likewise comprise 81 wt% S. Following the established procedure for RASP,[47] DDP and sulfur were thus heated to 230 °C in a 30 : 70 mass ratio for 24 h (Scheme 3). This is a higher reaction temperature than is used in inverse vulcanization because the aryl halide monomer in RASP is less reactive than the olefins used in inverse vulcanization. As the components were heated, the colour first changed from yellow (molten sulfur) to the brown-red colour characteristic of polymeric sulfur radicals. Eventually, the colour changed to a dark, nearly black colour. When the dark, viscous liquid was cooled to room temperature it became a glassy solid (**XS81**) having the dark brown-orange colour characteristic of polymeric sulfur (Figure 1).

Many HSMs are composites wherein sulfur – trapped in orthorhombic, oligomeric or polymeric form – is comingled with the network of organic units that are crosslinked with sulfur chains. The established way to quantify the amount of sulfur that is not covalently incorporated into the cross-linked material is to fractionate the material using carbon disulfide.[13, 15, 27] Orthorhombic sulfur is readily soluble in $CS_2$, whereas cross-linked organosulfur networks generally are not. **XS81** was thus fractionated in $CS_2$ to give a soluble and insoluble fraction. The soluble fraction accounted for 57% of the total mass of **XS81**, and was >99% sulfur, as confirmed by elemental analysis. From the aforementioned analyses, the number of sulfur atoms in the crosslinked fraction, as well as the number of crosslinked carbon atoms are both known. This information allowed calculation of the average crosslinking chain in **XS81** to be comprised by ≤ 4 sulfur atoms. The sulfur crosslinks in **XS81** are

A)



B)



C)
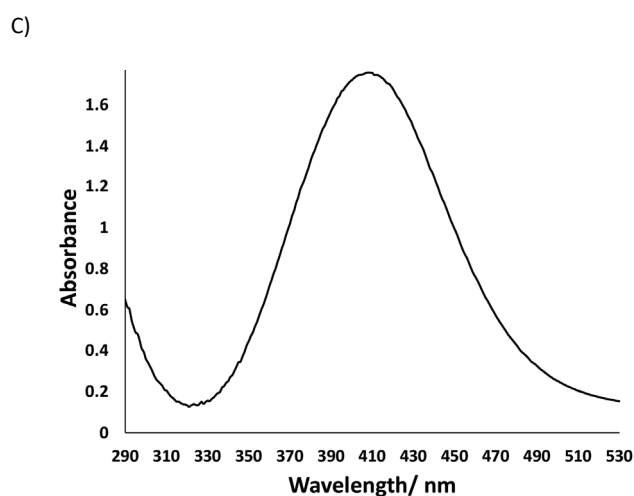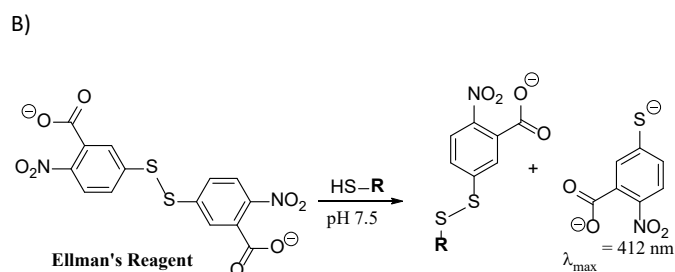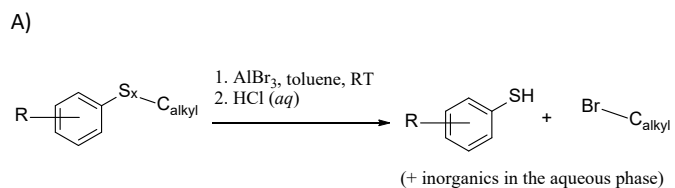


**Scheme 4**. A) The reaction of $AlBr_3$ with organosulfur compounds. B) The reaction of Ellman's reagent with aryl thiols to give a colorimetric response. C) UV spectrum from Ellman's analysis of products resulting from depolymerization of **XS81** by reaction with $AlBr_3$.

somewhat shorter than the average length of cross-links in HSMs prepared by inverse vulcanization of cellulose (40 S atoms)[28] or lignin (76 S atoms),[27] but comparable to those prepared from tyrosine (five S atoms)[15] or polystyrene derivatives (five S atoms).[13] Some caution should be exercised in the direct comparison of crosslinker length, however, because the number of available sites for crosslinking differ from material to material. Despite the presence of free, extractable sulfur in **XS81**, no phase separation was observed in the material. Scanning electron microscopy (SEM) imaging with element mapping by energy dispersive X-ray analysis (EDX) confirmed the uniform distribution of sulfur, carbon and oxygen in the materials (Figures S5-6 in the ESI) and that the surface elemental analysis is consistent with the bulk composition from combustion analysis (Figure S7 in the ESI).

The integrity of the DDP-derived repeat unit in the composite was confirmed by infrared (IR) spectroscopy (spectra are provided in the ESI). Characteristic peaks attributable to DDP were retained in spectra of both the polymer and the $CS_2$-insoluble fraction, as manifested by peaks at 844 cm$^{-1}$ (out of-plane aromatic C–H deformation), 1354 cm$^{-1}$ (C–H stretching), 1165 (C–O stretching) and peaks near 1573 cm$^{-1}$ (aromatic C=C stretching). Peaks at 584 and 705 cm$^{-1}$, attributable to C–Cl stretches, are diminished in the spectrum for **XS81** as compared to the spectrum for DDP, further confirming the replacement of chloride substituents expected of the RASP mechanism (Figures S1–2 in the ESI). The attenuation of C–Cl stretches is accompanied by the emergence of new bands in the spectrum of **XS81** at 605-620 cm$^{-1}$, attributable to C–S stretches from the new bonds formed during RASP.

As indicated in Scheme 2, the chlorine is initially removed as $S_2Cl_2$. Caution should be exercised when performing the RASP reaction because $S_2Cl_2$ is highly toxic. Some of the $S_2Cl_2$ is expected to react with the phenolic sites. In an effort to quantify the generation of $S_2Cl_2$ released rather than reacting *in situ*, the reaction was performed in a Schlenk flask vented to a water reservoir where outgassed $S_2Cl_2$ would be hydrolysed to HCl. The pH of the water solution fell predictably, and a significant quantity of HCl was collected by this method. However, tubing, grease and septa of the apparatus discoloured as well, indicating reaction with $S_2Cl_2$. Stainless steel and fluoropolymer tubing were also discoloured in subsequent trials, so the exact quantity of $S_2Cl_2$ generated could not be accurately quantified. It would be expected that the reaction done in the sealed tube would facilitate reaction of the $S_2Cl_2$ with the phenolic sites to a greater extent than when the reaction is carried out in an open or nitrogen-purged vessel, so the pressure tube reaction appears to be the safest approach to avoid $S_2Cl_2$ release into the atmosphere. Although results of the trapping experiment are consistent with the established mechanism, contribution of other potential pathways ($S_NAr$ or EAS, for example) cannot be completely ruled out.

Pyun has demonstrated the aforementioned benzylic crosslinking by polymeric sulfur radicals previously.[11] This crosslinking is initiated by H-atom abstraction from the benzylic position by a sulfur radical. This ultimately leads to generation of $H_2S$. In an effort to quantify the upper limit on how many benzylic sites may be crosslinked in **XS81**, the H2S generated was trapped by bubbling gas generated first through water (where the $S_2Cl_2$ is hydrolysed as noted above) and then through an $AgNO_3$ solution, with which the $H_2S$ reacts to produce $Ag_2S$.[13] The $Ag_2S$ was then collected, dried and weighed. From this quantification, an upper limit for 17% of the benzylic sites to be crosslinked was established, assuming that every H atom released in the $H_2S$ derived from benzylic sites.

The depiction of **XS81** in Scheme 3 suggests crosslinking by the established benzyl site crosslinking mechanisms as well as by formation of direct S–$C_{aryl}$ bonds that are not known to form during inverse vulcanization. The loss of chloro substituents

**Table 1**. Thermal Properties Analysis

| Material | Sulfur | **XS81** |
|---|---|---|
| $T_d^{[a]}$ /°C | 228 | 245 |
| DSC $T_g$/°C | NA | −34 |
| DSC $T_m^{[b]}$/°C | 120 | 116 |
| $\Delta H_{cc}$ J/g | NA | 9 |
| $\Delta H_m$ J/g | 51 | 19 |
| %xtl [c] | 100 | 18 |

[a] The temperature at which the 5% mass loss was observed. [b] The temperature at the peak maxima of the endothermic melting peak [c]The percent crystallinity of each samples was calculated with respect to sulfur (normalized to 100%)

from aryl rings observed by IR spectroscopy and elemental analysis provide some indirect evidence for such bond formation. To more directly assess the extent to which S–$C_{aryl}$ bonds were present in **XS81**, a sample was first depolymerized by reaction with $AlBr_3$. Aluminium tribromide reacts with S–$C_{alkyl}$ bonds to produce Br–$C_{alkyl}$ bonds, but the S–$C_{aryl}$ bonds remain intact, producing aryl thiols after aqueous workup (Scheme 4A).[53, 54] Following depolymerization, the thiol concentration can be quantified by the Ellman's reagent method.[55, 56] Ellman's reagent is a colorimetric indicator that undergoes a specific reaction with thiols to produce a species having an absorption maximum at 412 nm (Figure 4B). Reacting depolymerization products with Ellman's reagent thus provides a facile way to assess total thiol content in the polymer by UV/vis spectroscopy. The absorbance of thiol species in the UV-vis spectrum resulting from Ellman's analysis of depolymerization products (Scheme 4C) is consistent with the aforementioned results of sulfur / chlorine elemental analysis of soluble / insoluble fractions. The agreement of elemental analysis and Ellman's analysis thus provides further substantiation for the hypothesis that each chlorine lost from the DDP monomer leads to the formation of exactly one S–$C_{aryl}$ bond. Furthermore, prior to depolymerization, **XS81** itself gives a negative Ellman's test for thiols, so the thiols detected cannot be attributable to surface or pre-existing thiols from the initial RASP reaction.

### Thermal and Morphological Properties

Having characterized structural aspects of the composite, the thermal, morphological and mechanical properties of **XS81** were evaluated. Thermogravimetric analysis (TGA, Table 1 and Figure 2) revealed that **XS81** had a higher char yield after heating to 800 °C than either of the two monomers, a common feature of high aromatic-content HSMs.[5, 12, 13, 57] The decomposition temperatures of DDP and sulfur are 90 °C and 228 °C, respectively. In contrast, **XS81** has two distinct decomposition temperatures events. The first decomposition event is attributable to decomposition of the entrapped sulfur and accounts for 59% of the material's mass, closely matching the amount of non-covalently incorporated sulfur quantified from $CS_2$ extraction (57%). The second decomposition event occurs at 470 °C (assigned from the local maximum of the
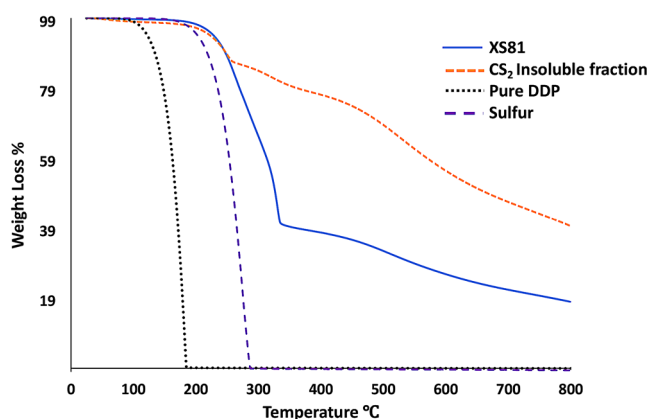
**Figure 2.** TGA traces for sulfur, pure DDP monomer, **XS81**, and CS₂-insoluble fraction of **XS81**.
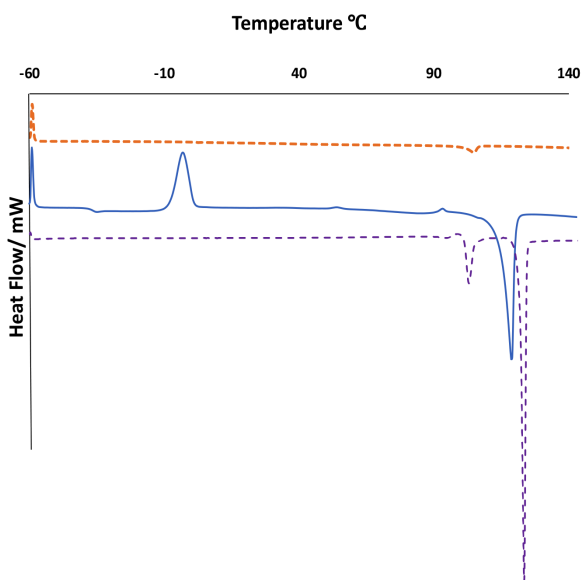


**Figure 3**. DSC data analysis of sulfur (lower dashed line), **XS81** (solid line), and CS₂-insoluble fraction of **XS81** (upper dashed line).

derivative curve) and corresponds to the expectedly high-temperature decomposition of the aryl-sulfide part of the composite. More evidence for assignment of the decomposition events was gained by subjecting the CS₂-insoluble fraction to TGA. The CS₂-insoluble fraction of **XS81** has had the unbound sulfur removed, so the decomposition attributable to sulfur domains is much smaller in the TGA trace for this fraction, while the subsequent degradation of organic materials is responsible for most of the mass loss.

Differential scanning calorimetry (DSC, Table 1 and Figure 3) analysis of **XS81** revealed an endothermic melting at 116 °C attributable to orthorhombic sulfur. This peak is notably diminished in the DSC analysis of the CS₂-insoluble fraction of

**Table 2**. Mechanical Properties of **XS81**

| Material | Sulfur | **XS81** |
|---|---|---|
| E' at −60 °C (MPa) | 373 | 633 |
| tan δ $T_g$ (°C) | NA[a] | 7 |
| E'' $T_g$ (°C) | NA[a] | −37, 4, 67 |
| flexural strength/modulus (MPa) | NA | 2.0/ 240 |

[a] No transitions were detected.

the material from which the orthorhombic sulfur has been removed (Figure 3). The heating curve exhibited a small glass transition at −35 °C attributed to the glass transition temperature of oligomeric / polymeric sulfur catenates. Orthorhombic sulfur itself has no $T_g$. Cold crystallization peaks at −3 and 92 °C are also observed for **XS81** attributable to an exothermic process resulting from partial organization of polymer chains and reflects the amorphous nature of **XS81**. Given the relationship between crystallinity and mechanical properties, the percent crystallinity was quantified by integrating cold crystallization enthalpies and melting enthalpies in DSC traces for **XS81**. From this analysis, **XS81** was found to exhibit only 18% as much crystallinity as the sulfur sample (Table 1), demonstrating effective stabilization of the majority of trapped sulfur, with only about 18% of the trapped sulfur in the orthorhombic form even after weeks of aging.

**Mechanical Properties.**

Dynamic mechanical analysis (DMA) was used to assess the viscoelastic properties of **XS81**. DMA data (Table 2) were first collected over the temperature range of −60 to +80 °C to assess the temperature-dependence of storage modulus (E'), loss modulus (E'') and damping factor (tanδ).

The peak maxima of the tanδ curve (Figure S3 in the ESI), at which the highest energy dissipation occurs, is at 7 °C and corresponds to the mechanical $T_g$ of the polymer. Three peak maxima were observed in the loss modulus curve. The peak at the lowest temperature can be attributed to β relaxations of the polymer as a result of intrinsic, non-constrained molecular motions in amorphous regions of the material.[58] The major transition given at 3 °C in the E'' curve is attributed to the glass transition temperature of the polymer as it resembles the major transition in tanδ curve and the steep drop in the E' curve. Transitions such as the one occurring at above 20 °C in both E' and E'' curves have been attributed to freedom of relative movement of chains in less-ordered regions of a polymer film.[58]

Stress-strain analysis of **XS81** at room temperature provides a practical snapshot of how the material might perform under typical operating conditions at close to standard room temperature (25 °C). Stress-strain analysis revealed that **XS81** has a flexural strength of 2.0 MPa, similar to or exceeding the flexural strength of some previous HSMs. The diisopropenyl

benzene (DIB)-sulfur copolymers require 50 wt.% of organic crosslinker to reach a similar flexural strength ($\leq$ 2.0 MPa) that is accomplished with only 19 wt.% DDP crosslinker in **XS81** prepared by RASP.[5] However, depending on the nature of the crosslinker, and the number of crosslinks, mechanical properties of the HSMs can be varied. We recently reported a flexural strength of 3.6 MPa for a chlorolignin-sulfur copolymer prepared by RASP and consisting of 19 wt % of organic crosslinker. A polymer made from a 1:1 mass ratio of dicyclopentadiene and sulfur has a much higher flexural strength of 6 MPa.[5]

One of the major issues of the current exterior building materials is that water absorption followed by freeze-thaw cycles causes fractures, thus lowering operational lifetime. Sulfur is quite hydrophobic, having a low critical surface energy of 27 mN/m. When a block of commercial Portland cement is submerged in water for 24 h, for example, it absorbs 28% of its mass in water. In contrast, a block of **XS81** takes up <0.5 wt.% of water after being submerged for 24 h. Another especially attractive feature of HSMs for potential commercial applications is the ease with which many of them can be processed and recycled by simple melt casting. **XS81** likewise can be subjected to many heating/recasting cycles while retaining its mechanical strength over at least a dozen cycles (Figure 4).
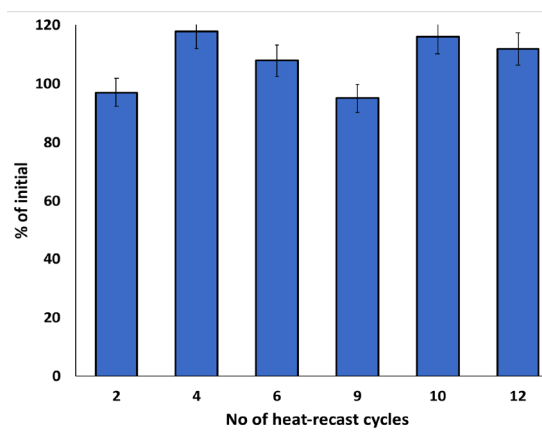


**Figure 4.** The mechanical strength of **XS81** is retained over at least a dozen break-melt-cast reprocessing cycles.

## Conclusions

The RASP route was employed to forms an HSM (**XS81**) by copolymerizing elemental sulfur with a small molecular dichloroxylenol derivative. **XS81** was characterized as a composite wherein the sulfur in is distributed between cross-linking chains and trapped polymeric sulfur that is not covalently attached to the network. The formation of S–C$_{aryl}$ bonds was demonstrated by a combination of IR spectroscopy, elemental analysis, depolymerization and Ellman's analysis by UV-vis spectroscopy. **XS81** is readily melt-processable and

retains its mechanical integrity over many heat-recast cycles. This is the first report of a HSM comprising stabilized polymeric sulfur that has been successfully prepared from a small molecular comonomer by RASP. This work thus demonstrates a new route to access HSMs using small molecular aryl halides, a notable expansion beyond the olefins required for the well-studied inverse vulcanization route to HSMs from small molecular comonomers.

## Experimental

### Chemicals and Materials

2,4-dimethyl-3,5-dichlorophenol and Carbon disulfide were purchased from Bean Town Chemicals. Sulfur powder (99.5%) was purchased from Alfa Aesar. **Tris**(hydroxymethyl)aminomethane hydrochloride and 5, 5'-Dithio-*bis*-(2-nitrobenzoic acid) were purchased from VWR Analytical. These chemicals were used without further purification unless otherwise noted.

### General Considerations

Thermogravimetric analysis (TGA) data were recorded on a Mettler Toledo 2STARe instrument over the range 20 to 800 °C, with a heating rate of 5 °C min$^{-1}$ under a flow of N$_2$ (100 mL min$^{-1}$). Differential scanning calorimetry (DSC) data was obtained using Mettler Toledo DSC 3 STAR$^e$ System, over the range of −60 to 140 °C, with a heating rate of 10 °C min$^{-1}$ under a flow of N$_2$ (200 mL min$^{-1}$). All the reported data were taken from the third heat/cool cycles. Melting enthalpies and the cold crystallization enthalpies were calculated using DSC data. The reduction of the percent crystallinity of XS81 with respect to sulfur was calculated using the following equation.

$$\Delta\chi_c = 1 - \left\{ \frac{\Delta H_{m(LS_x)} - \Delta H_{cc(LS_x)}}{\Delta H_{m(S)} - \Delta H_{cc(S)}} \right\} * 100\%$$

$\Delta\chi_c$      - Change of percentage crystallinity with respect to sulfur
$\Delta H_{m(LS_x)}$ - Melting enthalpy of composite materials (LS$_x$)
$\Delta H_{cc(LS_x)}$ - Cold crystallization enthalpy of composite materials (LS$_x$)
$\Delta H_{m(S)}$    - Melting enthalpy of sulfur
$\Delta H_{cc(S)}$    - Cold crystallization enthalpy of sulfur

Dynamic Mechanical Analysis (DMA) data was acquired using Mettler Toledo DMA 1 STAR$^e$ System in single cantilever mode. DMA samples cured for 120 h were cast from silicone resin moulds (Smooth-On Oomoo® 30 tin-cure). The sample dimensions were approximately 19×9×2 mm. The temperature range of –60 to 80 °C was used to obtain the temperature dependent data with a heating rate of 5 °C min$^{-1}$. The samples were so clamped with1 cN·m force and the results were collected with the measurement mode of displacement control with a displacement amplitude of 5 μm and a frequency of 1

Hz. The samples cured for 120 h prior to stress-strain analysis at room temperature. The samples were clamped under single cantilever mode. The force was varied from 0 to 10 N with a ramp rate of 0.1 N·min$^{-1}$. Fourier transform infrared spectra were obtained using a Shimadzu IR Affinity-1S instrument with ATR attachment, operating over the range of 400-4000 cm$^{-1}$ at ambient temperature. Cary 50-Bio UV-Vis Spectrophotometer was used to obtain the UV-Visible spectra, scanning from 800-200 nm.

### Synthesis of XS81

Elemental sulfur (70 wt%) was weighed directly into a pressure tube under inert environment. The tube was heated to 180 °C in an oil bath over which time the sulfur melted. Once the sulfur turned a viscous dark red-orange color (indicative of thermal ring-opening), 30 wt% of 2,4-dimethyl-3,5-dichlorophenol was slowly added to the molten sulfur. Then the temperature was gradually increased to 230°C and heating was continued for 24 h with continuous stirring with a magnetic stir bar. The whole procedure was done under $N_2$ gas. The prepared aryl halide-sulfur combination was subjected to elemental combustion microanalysis.

*CAUTION: Heating elemental sulfur with organics can result in the formation of $H_2S$ gas. $H_2S$ is toxic, foul-smelling, and corrosive. This reaction may also produce $S_2Cl_2$, a toxic and reactive material.*

*CAUTION: Heating material in a sealed tube can generate high pressures. Use caution and consult the manufacturer of the pressure apparatus used for safety guidance*

### Depolymerization with AlBr$_3$

The XS81 sample (, 30 mg) so powdered was mixed with 60 mg of AlBr$_3$ in a glovebox. The mixture of solid was dissolved in 6 mL of anhydrous toluene in $N_2$ environment for 72 h. At the end of the reaction time, the solvent was filtered and 5% (v/v) HCl: ethanol 5 mL was added. Following three consecutive washes, the organic layer was separated out.
.

### The Procedure for the reaction of Aryl thiols with Ellman's reagent

The procedure was carried out according to a known method with slight changes. The stock solution of DTNB (5, 5'-Dithio-*bis*-(2-nitrobenzoic acid) was prepared by dissolving 40 mg of DTNB in 10 mL of DMSO. The solution was 100-fold diluted into 0.1 mM DTNB solution using Tris HCl (*Tris*(hydroxymethyl)aminomethane hydrochloride) buffer solution at pH 7.4. 1mL of the solution containing depolymerized products and 19 mL of 0.1 mM DTNB were mixed together and let it to sit for 2 minutes at room temperature. The samples were then analysed through UV-vis spectrophotometer by using 10% (v/v) Tris HCl: DTNB solution as the blank. The same procedure was carried out without adding AlBr$_3$ to confirm the absence of thiol groups in the initial sample.

## Conflicts of interest

There are no conflicts to declare.

## Acknowledgements

## Notes and references

1. W. J. Chung, J. J. Griebel, E. T. Kim, H. Yoon, A. G. Simmonds, H. J. Ji, P. T. Dirlam, R. S. Glass, J. J. Wie, N. A. Nguyen, B. W. Guralnick, J. Park, A. Somogyi, P. Theato, M. E. Mackay, Y.-E. Sung, K. Char and J. Pyun, *Nat Chem*, 2013, **5**, 518-524.

2. J. M. Chalker, M. J. H. Worthington, A. L. Nicholas and J. E. Louisa, *Top Curr Chem (Cham)*, 2019, **377**, 16.

3. D. A. Boyd, *Angew Chem Int Ed Engl*, 2016, **55**, 15486-15502.

4. M. J. H. Worthington, R. L. Kucera and J. M. Chalker, *Green Chem.*, 2017, **19**, 2748-2761.

5. T. Hasell, J. Smith, S. Green, S. Petcher, D. Parker, B. Zhang, M. J. H. Worthington, X. Wu, C. Kelly, T. Baker, C. Gibson, J. Campbell, D. Lewis, M. Jenkins, H. Willcock and J. M. Chalker, *Chem. - Eur. J.*, 2019, **25**, 10433-10440.

6. D. J. Parker, H. A. Jones, S. Petcher, L. Cervini, J. M. Griffin, R. Akhtar and T. Hasell, *J. Mater. Chem. A*, 2017, **5**, 11682-11692.

7. Y. Zhang, N. G. Pavlopoulos, T. S. Kleine, M. Karayilan, R. S. Glass, K. Char and J. Pyun, *J. Polym. Sci., Part A Polym. Chem.*, 2019, **57**, 7-12.

8. H.-K. Lin, Y.-S. Lai and Y.-L. Liu, *ACS Sustainable Chem. Eng.*, 2019, **7**, 4515-4522.

9. J. Wreczycki, D. M. Bielinski and R. Anyszka, *Polymers (Basel, Switz.)*, 2018, **10**, 870/871-870/820.

10. Y. Zhang, K. M. Konopka, R. S. Glass, K. Char and J. Pyun, *Polym. Chem.*, 2017, **8**, 5167-5173.

11. Y. Zhang, J. J. Griebel, P. T. Dirlam, N. A. Nguyen, R. S. Glass, M. E. MacKay, K. Char and J. Pyun, *J. Polym. Sci., Part A: Polym. Chem.*, 2017, **55**, 107-116.

12. S. Diez, A. Hoefling, P. Theato and W. Pauer, *Polymers (Basel, Switz.)*, 2017, **9**, 59/51-59/16.

13. T. Thiounn, M. K. Lauer, M. S. Bedford, R. C. Smith and A. G. Tennyson, *RCS Advances*, 2018, **8**, 39074-39082.

14. C. Herrera, J. Ysinga Kristen and L. Jenkins Courtney, *ACS Appl Mater Interfaces*, 2019, **11**, 35312-35318.

15. T. Thiounn, A. G. Tennyson and R. C. Smith, *RSC Advances*, 2019, **9**, 31460-31465.

16. M. Mann, J. E. Kruger, F. Andari, J. McErlean, J. R. Gascooke, J. A. Smith, M. J. H. Worthington, C. C. C. McKinley, J. A. Campbell, D. A. Lewis, T. Hasell, M. V. Perkins and J. M. Chalker, *Org. Biomol. Chem.*, 2019, **17**, 1929-1936.

17. N. A. Lundquist, M. J. H. Worthington, N. Adamson, C. T. Gibson, M. R. Johnston, A. V. Ellis and J. M. Chalker, *RSC Adv.*, 2018, **8**, 1232-1236.

18. A. Hoefling, Y. J. Lee and P. Theato, *Macromol. Chem. Phys.*, 2017, **218**, n/a.

19. X. Qin, Y. He, S. Khan, B. Zhang, F. Chen, D. Dong, Z. Wang and L. Zhang, *ACS Sustainable Chem. Eng.*, 2018, **6**, 12865-12871.

20. S. F. Valle, A. S. Giroto, R. Klaic, G. G. F. Guimaraes and C. Ribeiro, *Polym. Degrad. Stab.*, 2019, **162**, 102-105.

21. M. J. H. Worthington, C. J. Shearer, L. J. Esdaile, J. A. Campbell, C. T. Gibson, S. K. Legg, Y. Yin, N. A. Lundquist, J.

R. Gascooke, I. S. Albuquerque, J. G. Shapter, G. G. Andersson, D. A. Lewis, G. J. L. Bernardes and J. M. Chalker, *Advanced Sustainable Systems*, 2018, **2**, 1800024.

22. M. J. H. Worthington, R. L. Kucera, I. S. Albuquerque, C. T. Gibson, A. Sibley, A. D. Slattery, J. A. Campbell, S. F. K. Alboaiji, K. A. Muller, J. Young, N. Adamson, J. R. Gascooke, D. Jampaiah, Y. M. Sabri, S. K. Bhargava, S. J. Ippolito, D. A. Lewis, J. S. Quinton, A. V. Ellis, A. Johs, G. J. L. Bernardes and J. M. Chalker, *Chem. - Eur. J.*, 2017, **23**, 16106.

23. A. D. Smith, T. Thiounn, E. W. Lyles, E. K. Kibler, R. C. Smith and A. G. Tennyson, *Journal of Polymer Science Part A*, 2019, **57**, 1704-1710.

24. M. P. Crockett, A. M. Evans, M. J. H. Worthington, I. S. Albuquerque, A. D. Slattery, C. T. Gibson, J. A. Campbell, D. A. Lewis, G. J. L. Bernardes and J. M. Chalker, *Angew. Chem., Int. Ed.*, 2016, **55**, 1714-1718.

25. C. Fu, G. Li, J. Zhang, B. Cornejo, S. S. Piao, K. N. Bozhilov, R. C. Haddon and J. Guo, *ACS Energy Lett.*, 2016, **1**, 115-120.

26. A. Hoefling, D. T. Nguyen, Y. J. Lee, S.-W. Song and P. Theato, *Mater. Chem. Front.*, 2017, **1**, 1818-1822.

27. M. S. Karunarathna, M. K. Lauer, T. Thiounn, R. C. Smith and A. G. Tennyson, *J. Mater. Chem. A*, 2019, **7**, 15683-15690.

28. M. K. Lauer, T. A. Estrada-Mendoza, C. D. McMillen, G. Chumanov, A. G. Tennyson and R. C. Smith, *Advanced Sustainable Systems*, 2019, DOI: 10.1002/adsu.201900062.

29. S. Namnabat, J. J. Gabriel, J. Pyun, R. A. Norwood, E. L. Dereniak and J. van der Laan, *Proc. SPIE*, 2014, **9070**, 90702H/90701-90702H/90707.

30. J. J. Griebel, S. Namnabat, E. T. Kim, R. Himmelhuber, D. H. Moronta, W. J. Chung, A. G. Simmonds, K.-J. Kim, J. van der Laan, N. A. Nguyen, E. L. Dereniak, M. E. MacKay, K. Char, R. S. Glass, R. A. Norwood and J. Pyun, *Adv. Mater. (Weinheim, Ger.)*, 2014, **26**, 3014-3018.

31. Z. Chen, J. Droste, G. Zhai, J. Zhu, J. Yang, M. R. Hansen and X. Zhuang, *Chem. Commun. (Cambridge, U. K.)*, 2019, **55**, 9047-9050.

32. F. Zhao, Y. Li and W. Feng, *Small Methods*, 2018, **2**, 1-34.

33. A. M. Abraham, S. V. Kumar and S. M. Alhassan, *Chem. Eng. J. (Amsterdam, Neth.)*, 2018, **332**, 1-7.

34. S. Akay, B. Kayan, D. Kalderis, M. Arslan, Y. Yagci and B. Kiskan, *J. Appl. Polym. Sci.*, 2017, **134**, n/a.

35. T. Hasell, D. J. Parker, H. A. Jones, T. McAllister and S. M. Howdle, *Chem. Commun. (Cambridge, U. K.)*, 2016, **52**, 5383-5386.

36. *Journal*, 1978.

37. R. Gregor and A. Hackl, *Adv. Chem. Ser.*, 1978, **165**, 54-78.

38. W. C. McBee and T. A. Sullivan, *Adv. Chem. Ser.*, 1978, **165**, 135-160.

39. A. H. Vroom, *Polym. Concr., Int. Congr., 7th*, 1992, 606-621.

40. S. Yu, H. Kwon, H. R. Noh, B.-I. Park, N. K. Park, H.-J. Choi, S.-C. Choi and G. D. Kim, *RSC Adv.*, 2015, **5**, 36030-36035.

41. M. M. K. Ksiazek, *Anti-Corros. Methods Mater.*, 2017, **64**, 1-15.

42. B. T. Michal, C. A. Jaye, E. J. Spencer and S. J. Rowan, *ACS Macro Lett.*, 2013, **2**, 694-699.

43. J. J. Griebel, N. A. Nguyen, S. Namnabat, L. E. Anderson, R. S. Glass, R. A. Norwood, M. E. MacKay, K. Char and J. Pyun, *ACS Macro Lett.*, 2015, **4**, 862-866.

44. A. J. R. Amaral and G. Pasparakis, *Polym. Chem.*, 2017, **8**, 6464-6484.

45. M. Arslan, B. Kiskan and Y. Yagci, *Scientific Reports*, 2017, **7**, 1-11.

46.  A. Takahashi, R. Goseki, K. Ito and H. Otsuka, *ACS Macro Lett.*, 2017, **6**, 1280-1284.
47.  M. S. Karunarathna, A. G. Tennyson and R. C. Smith, *Journal of Materials Chemistry A*, 2020, **8**, 548-553.
48.  S. H. Je, H. J. Kim, J. Kim, J. W. Choi and A. Coskun, *Adv. Funct. Mater.*, 2017, **27**, 1703947.
49.  S. H. Je, O. Buyukcakir, D. Kim and A. Coskun, *Chem*, 2016, **1**, 482-493.
50.  J. M. Lee, G. Y. Noh, B. G. Kim, Y. Yoo, W. J. Choi, D.-G. Kim, H. G. Yoon and Y. S. Kim, *ACS Macro Lett.*, 2019, **8**, 912-916.
51.  US3633A, 1844.
52.  B. Hortling, *Die Makromolekulare Chemie*, 1977, **178**, 2185-2196.
53.  D. S. Tarbell and D. P. Harnish, *Chem. Rev. (Washington, DC, U. S.)*, 1951, **49**, 1-90.
54.  D. P. Harnish and D. S. Tarbell, *J. Am. Chem. Soc.*, 1948, **70**, 4123-4127.
55.  D. P. Harnish and D. S. Tarbell, *J. Am. Chem. Soc.*, 1948, **70**, 4123-4127.
56.  P. Eyer, F. Worek, D. Kiderlen, G. Sinko, A. Stuglin, V. Simeon-Rudolf and E. Reiner, *Analytical Biochemistry*, 2003, **312**, 224-227.
57.  M. Arslan, B. Kiskan and Y. Yagci, *Macromolecules*, 2016, **49**, 767-773.
58.  Z. Liu, P. Maréchal and R. Jérôme, *Polymer*, 1997, **38**, 4925-4929.